Materials Science and Engineering A 510–511 (2009) 224–228

Contents lists available at ScienceDirect

Materials Science and Engineering A

journal homepage: www.elsevier.com/locate/msea

Finding critical damage locations by Λ-filtering in finite-element modelling of a girth weld

Stefan Holmström*, Anssi Laukkanen, Kim Calonius

VTT Technical Research Centre of Finland, Kemistintie 3, Espoo, P.O. Box 1000, FI-02044 VTT, Finland

ARTICLE INFO

Article history:
Received 28 February 2008
Received in revised form 17 April 2008
Accepted 30 April 2008

Keywords:
Creep damage
Modelling
Constraint
FEA
Welds

ABSTRACT

In structures with uniform material properties, time dependent creep damage will develop in locations where the stress state is aggravated by triaxiality constraints. However, for non-uniform structures, such as welds, where several material zones (differing in microstructure and material properties) are present, the pin-pointing of the "weakest link" is even more challenging. For girth-welded pipes, the unfavourable conditions are known to be found in the vicinity of the heat-affected zone on the outer diameter. To find out how the triaxiality constraints influence accumulated "creep exhaustion", three girth welds simulated for different steels have been studied using the Λ-filtering technique. The Λ-filtering has been developed for finite element modelling for visualising the combined effect of creep ductility, creep rate and triaxiality constraint evolution assuming rigid plastic deformation for the stress triaxiality-dependent part. In this work, the creep response of three-zone girth welds was studied. In the case of the P23 steel, data for a real (experimental) consumable was used and for the others, assumption on creep strength and creep curve shapes was made according to material property ratios. The creep strain rate formulation used for this work is the logistic creep strain prediction model and its multiaxial implementation has been run in the Comsol multiphysics software package. The results of the weld simulations predict similar behaviour for the P22 and P91 welds, with assumed weld metal behaviour closer to the base material, and differing behaviour for the P23 with an overmatching (experimental) weld metal.

1. Introduction

The structural integrity of high temperature girth welds have been studied by many authors [1–10]. However, these studies mainly address the stress and strains in the different zones of the welds and are not taking the impact of triaxiality constraints and multiaxial creep ductility into account. This leads to simulation results where the locations of maximum stress or strain do not correspond to the locations where service-exposed girth welds actually develop creep damage. The influence of creep-ductility exhaustion under multiaxial conditions has been studied [11–13] and implemented in design codes [14–16] in recent years.

A new filtering technique (Λ-filtering [17]) has been defined based on a classical relation [18] for creep ductility ratio (uniaxial vs. multiaxial fracture strain) under complex stress loading assuming rigid plastic deformation. To visualise the creep exhaustion, the developed Λ-filter has been used together with the logistic creep strain prediction (LCSP) creep strain model for simulation of the girth welds of three steels, P23 [19], P22 [19] and P91 [20].

2. The strain model

The creep strain model, LCSP [21,22], is based on time to rupture and shape functions. This is also the models greatest strength since nearly the same robustness can be achieved for the strain model as for the rupture model. The LCSP model states that the full strain curves at specified temperature and stress can be acquired from knowing only the time to rupture and two material specific shape parameters p and x_0 (see Eqs. (1) and (2)).

The LCSP can be analytically differentiated and the resulting strain rate as a function of stress temperature and time to rupture can be written as

$$\dot{\varepsilon} = -\varepsilon\, k1\, k2\, x_0 \quad (1)$$

where ε (engineering strain) can be derived from the LCSP base equation, x_0 is one of the shape parameters and $k1$ and $k2$ are;

$$k1 = \frac{(LTF-1)^{1/p}}{p},$$

$$k2 = \frac{\log(t_r)+C}{(\log(t_\varepsilon)+C)^2 \cdot t_\varepsilon \cdot (LTF-1)} \quad \text{and} \quad LTF = \frac{\log(t_r)+C}{\log(t_\varepsilon)+C} \quad (2)$$

where t_r is the time to rupture, t_ε the time to strain ε, p the other shape parameter and C a constant ($C = 3.5$ in this work). An example

* Corresponding author. Tel.: +358 20 722 6890.
E-mail address: stefan.holmstrom@vtt.fi (S. Holmström).

0921-5093/$ – see front matter © 2008 Elsevier B.V. All rights reserved.
doi:10.1016/j.msea.2008.04.107

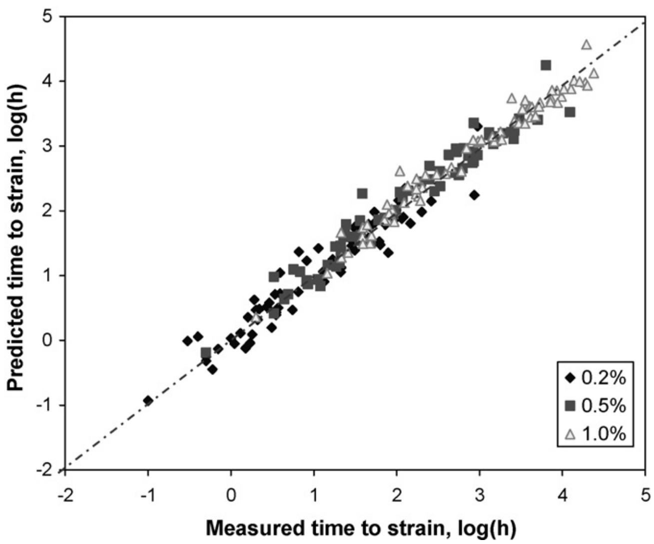

Fig. 1. Predicted vs. measured time to 0.2%, 0.5% and 1% creep strain for 4 heats of P91 [20], calculated on the basis of true rupture time and the shape parameters in Table 1.

of the fitting accuracy of the LCSP creep shape model is presented for P91 as measured vs. predicted time to specified strain (0.2, 0.5 and 1%) in Fig. 1. The presented multi-heat data is from the Japanese National Institute for Material Science (NIMS) data sheet [20]. The creep shape functions of the base material (BM) of P23, P22 and P91 steels are given in Table 1.

For the Comsol FE implementation the multiaxial LCSP creep strain rate expression has been attained from Eq. (1) (strain rate) by using a von Mises type flow rule and by deriving the expression for multiaxial creep strain rate (strain rate tensor) as follows:

$$\dot{\varepsilon}_{ij} = f(\varepsilon_u)(\delta\alpha_1 + \delta\alpha_2\beta(T) + \frac{3}{2}\alpha_3 s_{ij}) \quad (3)$$

where the first $f(\varepsilon_u)$ is a function of the uniaxial LCSP model (Eq. (1)), δ, α_i are constants, $\beta(T)$ a function of temperature and s_{ij} is the deviatoric stress tensor.

The FE implementation itself is formulated using a mixed FE approach for the strain rate and solution of the balance equations using the weighted Galerkin method. The FE equations are interpolated adaptively varying the order of polynomic interpolation basis from 2 to 5. Time integration of the rate equations is carried out using an implicit back differentiation routine, with variable step-size and order.

3. Visualizing multiaxial creep exhaustion by Λ-filtering

It is commonly known that for long term creep of pressure vessels (such as the welded pipe of this work) the maximum equivalent strains develop on the inner surface vessel, whereas the maximum equivalent stresses will redistribute towards the outer diameter due to creep. The multiaxial creep ductility again (due to triaxiality constraint) will be reduced towards the outer surface. Therefore, by filtering the acquired FE results of stress and strain by the expression for rigid plastic deformation;

$$\Lambda = \frac{\varepsilon_{fu}}{\varepsilon_{fm}} \cdot \varepsilon_m = \frac{1}{1.65\exp(-1.5\,h)}\varepsilon_m \quad (4)$$

where ε_{fu} is the uniaxial creep ductility, ε_{fm} the multaixial creep ductility and ε_m the local multiaxial creep strain and h is the hydrostatic stress over von Mises, an expression for "creep exhaustion" is attained. The background of the method lies in the classical Rice-Tracey model for growth of voids under a triaxial field of stress [23], i.e. the growth of voids is a function of stress triaxiality, and hence the ultimate failure strain of such a system is affected as well. The Rice-Tracey model is the simplest of available methods for incorporation of effects of stress triaxiality, but in any event it is an improvement in the interpretation of numerical results. Also, since the Λ-filter defined this way does not couple to the solution itself, it can be utilized as a straightforward separate post-processing method.

The filtering technique does not require local creep ductility values since it is expressed as ratio dependent on stress and momentary strain only. Theoretically if the Λ-values were to be divided by the correct local uniaxial creep ductility a normalized ratio of consumed multiaxial creep strain (or creep exhaustion), i.e. accumulated multiaxial strain over multiaxial fracture strain would be acquired.

Table 2
Simulation temperature for girth welds and predicted rupture time for base material (BM), crossweld (CW) and weld metal (WM). The values in brackets do not correspond to true data but to assumptions made for the specific zone.

	Material		
	P23	P22	P91
Temperature (°C)	595	550	625
t_r (BM) (h)	97,000	101,000	90,000
t_r (CW) (h)	70,000	(40,000)	(18,000)
t_r (WM) (h)	(280,000[a])	(100,000)	(90,000)

[a] B323B experimental consumable, life extrapolation with time factor 2.9, shape functions from for short-term test at 620 °C.

4. Assessed girth welds

Three girth welds have been simulated for P23, P22 and P91 steels for a welded pipe under a pressure of 139 bar equalling nominal Von-Mises stresses of 70 MPa. The temperature was selected to give about 100,000 h to rupture (see Table 2) for the corresponding base material. The welded pipe dimensions are 300 mm inner radius with a 28-mm wall thickness.

4.1. The creep properties for BM, HAZ and WM

For the successful simulation of the welded structure, in addition to models of expected rupture time also shape parameters are required. For the heat-affected zone (HAZ) it is assumed that the time to rupture is following a 20% reduction in strength (WSF = 0.8) and the shape of the creep curve takes this into account as an increased stress (σ/WSF replacing σ in shape equations of Table 1) as seen in Fig. 2. The weld material creep curve shapes for P23 are given by results acquired from creep testing of the strong but not very ductile experimental consumable B323B. For P91 and P22 the weld metal is assumed to be as strong as the base material (equal

Table 1
LCSP creep strain shape functions for P23, P22 and P91 steels (C = 3.5).

Material	x_0 (σ, T)	p (σ, T)
P23	$4.21 + 0.696\log\sigma - 7860/(T+273)$	$14.3–2.271\log\sigma - 4829/(T+273)$
P22	$-0.391 + 0.696\log\sigma - 3392.5/(T+273)$	$4.363–2.271\log\sigma + 3874.9/(T+273)$
P91	$-2.24 + 1.37\log\sigma - 3170/(T+273)$	$4.21–7.27\log\sigma + 14,200/(T+273)$